

Integrated source of tunable nonmaximally mode-entangled photons in a domain-engineered lithium niobate waveguide

Yang Ming, Zi-jian Wu, Guo-xin Cui, Ai-hong Tan, Fei Xu, and Yan-qing Lu

Citation: [Applied Physics Letters](#) **104**, 171110 (2014); doi: 10.1063/1.4874838

View online: <http://dx.doi.org/10.1063/1.4874838>

View Table of Contents: <http://scitation.aip.org/content/aip/journal/apl/104/17?ver=pdfcov>

Published by the [AIP Publishing](#)

Articles you may be interested in

[Review Article: Quasi-phase-matching engineering of entangled photons](#)

[AIP Advances](#) **2**, 041401 (2012); 10.1063/1.4773457

[Observation of quantum Talbot effect from a domain-engineered nonlinear photonic crystal](#)

[Appl. Phys. Lett.](#) **101**, 211115 (2012); 10.1063/1.4766728

[Monolithic integration of plasmonic waveguides into a complimentary metal-oxide-semiconductor- and photonic-compatible platform](#)

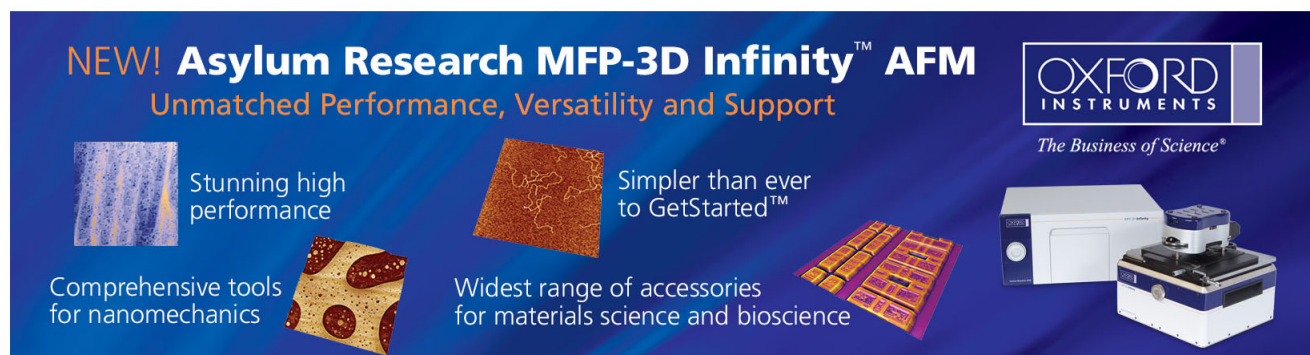
[Appl. Phys. Lett.](#) **96**, 121101 (2010); 10.1063/1.3365020

[Generation of continuous-wave broadband entangled beams using periodically poled lithium niobate waveguides](#)

[Appl. Phys. Lett.](#) **90**, 041111 (2007); 10.1063/1.2437057

[Nonlinear AlGaAs waveguide for the generation of counterpropagating twin photons in the telecom range](#)

[J. Appl. Phys.](#) **98**, 063103 (2005); 10.1063/1.2058197

This is a promotional banner for the Asylum Research MFP-3D Infinity AFM. The background is a dark blue gradient. At the top left, the text 'NEW! Asylum Research MFP-3D Infinity™ AFM' is written in white and orange, followed by the tagline 'Unmatched Performance, Versatility and Support' in orange. On the right side, the Oxford Instruments logo is displayed in white, with the slogan 'The Business of Science®' below it. The central part of the banner features four distinct images: a blue textured surface, a brown textured surface, a yellow and red patterned surface, and a photograph of the AFM instrument itself. Each image is accompanied by a short text description: 'Stunning high performance', 'Simpler than ever to GetStarted™', 'Comprehensive tools for nanomechanics', and 'Widest range of accessories for materials science and bioscience'.

Integrated source of tunable nonmaximally mode-entangled photons in a domain-engineered lithium niobate waveguide

Yang Ming,¹ Zi-jian Wu,¹ Guo-xin Cui,^{1,2} Ai-hong Tan,³ Fei Xu,^{1,a)} and Yan-qing Lu^{1,b)}

¹National Laboratory of Solid State Microstructures and College of Engineering and Applied Sciences, Nanjing University, Nanjing 210093, China

²Key Laboratory of Nanodevices and Nanoapplications, Suzhou Institute of Nano-Tech and Nano-Bionics, CAS, Suzhou 215000, China

³Laboratory for Quantum Information, China Jiliang University, Hangzhou 310018, China

(Received 6 April 2014; accepted 21 April 2014; published online 1 May 2014)

The nonmaximally entangled state is a special kind of entangled state, which has important applications in quantum information processing. It has been generated in quantum circuits based on bulk optical elements. However, corresponding schemes in integrated quantum circuits have been rarely considered. In this Letter, we propose an effective solution for this problem. An electro-optically tunable nonmaximally mode-entangled photon state is generated in an on-chip domain-engineered lithium niobate (LN) waveguide. Spontaneous parametric down-conversion and electro-optic interaction are effectively combined through suitable domain design to transform the entangled state into our desired formation. Moreover, this is a flexible approach to entanglement architectures. Other kinds of reconfigurable entanglements are also achievable through this method. LN provides a very promising platform for future quantum circuit integration.

© 2014 AIP Publishing LLC. [<http://dx.doi.org/10.1063/1.4874838>]

Entangled photon pairs are a crucial physical resource for quantum information science. Previously, the optical paths to generate and manipulate entangled photons have often been established through bulk optical elements.^{1,2} Thus, the performances of the photonic quantum circuits are inevitably affected during practical applications. For stable and high-quality quantum information processing, large-scale integrated quantum circuits are necessary.³ Owing to developments in optical waveguide technologies, several circuits have been designed to realize the fundamental functions of quantum optics.⁴⁻⁶

The nonmaximally entangled photon state (NEPS) is a special kind of entangled state that can be expressed as $(|A\rangle_1|B\rangle_2 \pm \varepsilon|B\rangle_1|A\rangle_2) / \sqrt{1+|\varepsilon|^2}$ or $(|A\rangle_1|A\rangle_2 \pm \varepsilon|B\rangle_1|B\rangle_2) / \sqrt{1+|\varepsilon|^2}$, where ε is not equal to 1.⁷ A and B could be variables such as polarization or frequency. The NEPS has important applications in remote state preparation⁸ and entanglement concentration,⁹ and it has been shown to be a better choice for multiple linear optical teleportation.¹⁰ This state has been generated in bulk quantum circuits.⁷ It would be very desired if the NEPS function also could be realized in integrated systems. However, there are no known schemes that can realize the corresponding function in silicon-based integrated systems, which have been adequately investigated in recent years.¹¹ The reason may be that silicon is not an effective $\chi^{(2)}$ nonlinear optical material, which limits its capability to control and modulate the generation process of entangled photons. However, generating the NEPS requires a flexible ability to modify the initial photon pairs provided by the spontaneous parametric down-conversion (SPDC) process.

As a solution to this problem, in this Letter, we propose a scheme to generate electro-optically tunable nonmaximally mode-entangled photon pairs in an integrated system based on a lithium niobate (LN) waveguide with suitably designed domain-engineered structures. LN is a multifunctional material, in which SPDC¹² and electro-optic (EO) effect¹³ could happen simultaneously. Initial photon pairs are generated through SPDC; and EO, which could be regarded as a two-photon interaction process, is utilized to modulate the quantum states of certain photons in the initial pairs to transform the entangled state into a desired form.¹⁴ Also, it is convenient to build waveguides in LN through the Ti-diffused approach, which offer well-defined discrete spatial modes.¹⁵ Based on these considerations, mode-entangled photon pairs could be generated and manipulated via proper domain engineering to combine SPDC and EO processes flexibly. Compared with the widely investigated polarization-entangled photon pair, this kind of entangled pair shows a higher brightness and generation rate.^{16,17}

We design the nonmaximally mode-entangled pair source based on a domain-engineered z -cut, x -propagating LN waveguide. The sketch of the device is shown in Fig. 1. To design the spatial mode entanglement, we carefully utilize the polarization characteristics of LN. The device consists of two different regions. Region I has a single domain period. This region is used to modulate the ratio of o -polarized to e -polarized photons in the pump light. As we discuss below, the e -polarized and o -polarized photons are used to generate the two respective eigenvectors of the entangled state. For a fixed pump wavelength, if the mismatch of the propagation constants β_o and β_e is well compensated through the periodically poled structure, the optical powers of o -polarized and e -polarized light could interchange effectively through applying a voltage to excite the EO interaction.¹³ As the EO coupling coefficient is

^{a)}Electronic mail: feixu@nju.edu.cn.

^{b)}Electronic mail: yqlu@nju.edu.cn.

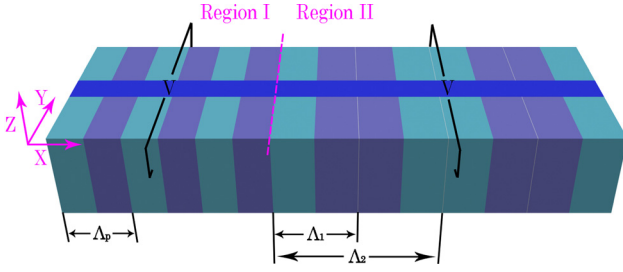


FIG. 1. Sketch of a tunable nonmaximally mode-entangled source. The blue sections represent positive domains, while the purple sections represent negative domains. Region I has a single modulation period Λ_p . Region II is poled with dual periods, namely, Λ_1 and Λ_2 . The modulation function is expressed as $f(x) = \text{sign}[\cos(2\pi x/\Lambda_1)] \times \text{sign}[\cos(2\pi x/\Lambda_2)]$.

linear with respect to the applied voltage, the ratio of field amplitudes of the e -polarized and o -polarized light on the output port of region I could be correspondingly modulated. Thus, the parameter ε of the entangled state is determined by the voltage applied to region I. Region II of the waveguide is poled with dual-periods. The basic modulation function is expressed as $f(x) = \text{sign}[\cos(2\pi x/\Lambda_1)] \times \text{sign}[\cos(2\pi x/\Lambda_2)]$. The x -direction corresponds to the propagation direction, while Λ_1 and Λ_2 represent the two periods. In this region, the photons undergo three interaction processes to form the nonmaximal spatial mode entanglement, including two SPDC processes and an EO interaction. Limited by the polarization-dependent character of the nonlinear coefficient, we utilize the SPDC processes based on the d_{31} component. They are $1_{p,e} \rightarrow 1_{s,o} + 0_{i,o}$, $1_{p,o} \rightarrow 0_{s,e} + 1_{i,o}$, where p , s , and i represent the pump, signal, and idler photons, respectively, while $o(e)$ denotes the polarization state and $0(1)$ corresponds to the order of the waveguide mode. To prevent the generated photons from being distinguished through polarization states, an EO interaction process is added, namely, $0_{s,e} \rightarrow 0_{s,o}$. Finally, the output photon pair is in $(1_{s,o}, 0_{i,o})$ or $(0_{s,o}, 1_{i,o})$. As the ratio of the e - and o -polarized 1st-order pump modes could be controlled in region I, the amplitudes of the two eigenvectors are easy to modulate. Through an appropriate choice of Λ_1 and Λ_2 , the phase mismatches of these processes could be compensated simultaneously by the equivalent reciprocal vector; thus, the entangled photons could be generated effectively.

The phase mismatches of the three processes mentioned above are written as

$$\begin{aligned}\Delta\beta_1 &= \beta_{p,e,1} - \beta_{s,o,1} - \beta_{i,o,0}, \\ \Delta\beta_2 &= \beta_{p,o,1} - \beta_{s,e,0} - \beta_{i,o,1}, \\ \Delta\beta_3 &= \beta_{s,o,0} - \beta_{s,e,0}.\end{aligned}\quad (1)$$

In the equations, $\beta_{j,\sigma,m}$ ($j=p, s, i$; $\sigma=o, e$; and $m=0, 1$) refers to the propagation constant of the corresponding waveguide mode, which is obtained based on Ref. 15. $\Delta\beta_1$ and $\Delta\beta_2$ correspond to two SPDC processes, while $\Delta\beta_3$ corresponds to the EO interaction. The inverted domains of the PPLN make the signs of the nonlinear coefficient d and the EO coefficient γ change periodically. The corresponding expressions for these coefficients are $d(x) = d_{31}f(x)$ and $\gamma(x) = \gamma_{51}f(x)$. The effective component of d and γ in our

situation are d_{31} and γ_{51} , respectively. Through Fourier transformation, they could be expressed as

$$\begin{aligned}d(x) &= d_{31} \sum_{m,n} G_{m,n} e^{iK_{m,n}x} \\ \gamma(x) &= \gamma_{51} \sum_{m,n} G_{m,n} e^{iK_{m,n}x}\end{aligned}\quad (2)$$

with

$$\begin{aligned}G_{m,n} &= \frac{4}{mn\pi^2} \sin\left(\frac{m\pi}{2}\right) \sin\left(\frac{n\pi}{2}\right) \\ K_{m,n} &= \frac{2m\pi}{\Lambda_1} + \frac{2n\pi}{\Lambda_2},\end{aligned}$$

where $K_{m,n}$ is the reciprocal vector for compensating the phase mismatch, with a corresponding Fourier coefficient of $G_{m,n}$. Λ_1 and Λ_2 represent the two modulation periods.

Through detailed calculations, we find an appropriate set of solutions. The width and depth of the waveguide core are both set to $10 \mu\text{m}$, and the maximum of the index difference is assumed to be 0.03. The pump, signal, and idler wavelengths are chosen to be $0.6050 \mu\text{m}$, $1.0169 \mu\text{m}$, and $1.4936 \mu\text{m}$, respectively. The operation temperature is 25°C . The corresponding values for the (m, n) series of $K_{m,n}$ are $\{(m_1, n_1) = (1, -3), (m_2, n_2) = (3, 1), \text{ and } (m_3, n_3) = (1, 1)\}$. Thus, we have $\Lambda_1 = 19.60 \mu\text{m}$ and $\Lambda_2 = 38.96 \mu\text{m}$, while the period Λ_p of region I is $7.79 \mu\text{m}$. The duty cycles of all these periods are equal to 0.5, as is shown in Fig. 1. It is worth noticing that the ratio Λ_2/Λ_1 is equal to 2, which creates a special situation. For region II, if we neglect the first and the last domains, the remaining portions have only one poled period. However, due to these two defects, the overall translational symmetry has been changed, and a new set of reciprocal vectors are introduced into the system. As the structural complexity is reduced, this design is better suited to practical realization. Moreover, the phase-matching conditions could be adjusted by the pump wavelength and the signal wavelength, which are shown in Fig. 2. The quantity $\Delta(\lambda)$ shown in the figures is defined as follows: we make $K_{1,-3}$ and $K_{3,1}$ equal to $\Delta\beta_1$ and $\Delta\beta_2$, respectively; then values for Λ_1 and Λ_2 can be obtained. Thus, we have $\Delta(\lambda) = \Delta\beta_3(\lambda) - K_{1,1}$. When $\Delta(\lambda) = 0$, $\Delta\beta_1$, $\Delta\beta_2$, and $\Delta\beta_3$ can be compensated simultaneously.

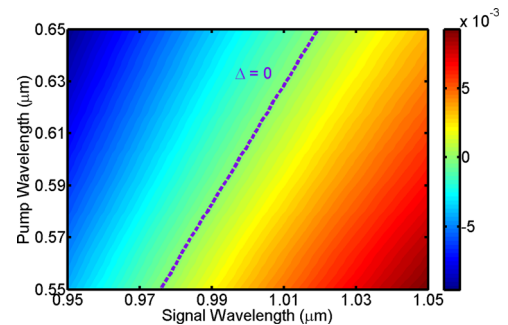


FIG. 2. Contour plot representation of the phase mismatch, i.e., $\Delta(\lambda)$. When $\Delta(\lambda) = 0$, three phase-matching conditions can be satisfied simultaneously. The values of $\Delta(\lambda)$ change with the signal wavelength and the pump wavelength. The purple dotted line corresponds to $\Delta(\lambda) = 0$. From the $\Delta(\lambda) = 0$ line, suitable phase-matching conditions can be chosen.

To obtain a quantum-mechanical description, we derive the state vector of the entangled photons through the effective Hamiltonian. In this derivation, the pump field is treated as an undepleted classical wave, while the signal and idler fields are quantized and represented by field operators. Based on the rotating wave approximation, we obtain H_{SPDC} as (3)

$$H_{SPDC} = -\frac{\hbar d_{31} E_{p1}}{2} \int \int d\omega_s d\omega_i [C_{110} F_{110} a_{s1}^\dagger a_{i0}^\dagger e^{-i(\omega_p - \omega_s - \omega_i)t} + \xi C_{101} F_{101} a_{s0}^\dagger a_{i1}^\dagger e^{-i(\omega_p - \omega_s - \omega_i)t} + H.C.] \quad (3)$$

In this equation, ξ is the ratio of field amplitudes of the o -polarized light to e -polarized light. Also, $C_{110} = G_{1,-3} h(L\Delta\beta_{110}) \sqrt{\omega_s \omega_i / n_{s1}^2 n_{i0}^2 N_{s1} N_{i0}}$ and $C_{101} = G_{3,1} h(L\Delta\beta_{101}) \sqrt{\omega_s \omega_i / n_{s0}^2 n_{i1}^2 N_{s0} N_{i1}}$, where $\Delta\beta_{110} = \Delta\beta_1 - K_{1,-3}$ and $\Delta\beta_{101} = \Delta\beta_2 - K_{3,1} \cdot N_{s1}, N_{i0}, N_{s0}$, and N_{i1} are normalization parameters of the corresponding modes, while n_{s1}, n_{i0}, n_{s0} , and n_{i1} are the refractive indices. E_{p1} is determined by the pump field. The values $h(L\Delta\beta_{110})$ and $h(L\Delta\beta_{101})$ are from the function of the form $h(x) = \exp(-ix/2) \text{sinc}(x/2)$. F_{110} and F_{101} are the overlap integrals of the corresponding normalized transverse mode profiles, which are defined as $F_{110} = \int dy dz \Psi_{p1(e)} \Psi_{s1} \Psi_{i0}$ and $F_{101} = \int dy dz \Psi_{p1(o)} \Psi_{s0} \Psi_{i1}$. Here, $\Psi(\vec{r})$ refers to the mode profile. Starting from a vacuum input, the biphoton state is derived as

$$|\varphi\rangle = -\frac{i}{\hbar} \int_{-\infty}^{\infty} dt H_{SPDC}(t) |0\rangle = \int d\nu [\Gamma_{110} |1_s, 0_i\rangle + \xi \Gamma_{101} |0_s, 1_i\rangle], \quad (4)$$

where $\Gamma_{110} = (id_{31} E_{p1}/2) C_{110} F_{110}$ and $\Gamma_{101} = (id_{31} E_{p1}/2) C_{101} F_{101}$. Also, due to the temporal integration, we have $\int \exp[-i(\omega_p - \omega_s - \omega_i)t] = \delta(\omega_p - \omega_s - \omega_i)$. Thus, the frequency integration based on ω_i could be eliminated. Moreover, we set $\omega_s = \Omega_s + \nu$. Here, Ω_s corresponds to the perfect phase-matching frequency, and ν is the natural bandwidth.

If we set the length of region II to 5 cm, the natural bandwidths of the two SPDC processes are calculated to be 0.20 nm and 0.19 nm, respectively. The bandwidths are so narrow that we could consider the case of a perfectly phase-matched output entangled state instead of that expressed by Eq. (4) to investigate the properties of the entangled source. Moreover, to ensure the validity of the process $0_s, e \rightarrow 0_s, o$, we perform relevant calculations based on the coupled wave equations for the EO effect¹³ and SPDC.¹⁸ The average pump power is set to 10 W, while the length of region II is also set to 5 cm. When the applied field is 1.5×10^5 V/m, for $\xi = 0.1, 1$, and 10, the ratio $P_{so}/(P_{se} + P_{so})$, representing the transformation efficiency, is equal to 0.9920, 0.9928, and 0.9932. That means that the photon could be effectively transformed into an o -polarized state. Based on the analyses above, the entangled state generated by our source could be finally simplified to

$$|\varphi\rangle = \frac{1}{\sqrt{1 + \varepsilon^2}} (|1_s, 0_i\rangle + \varepsilon |0_s, 1_i\rangle), \quad (5)$$

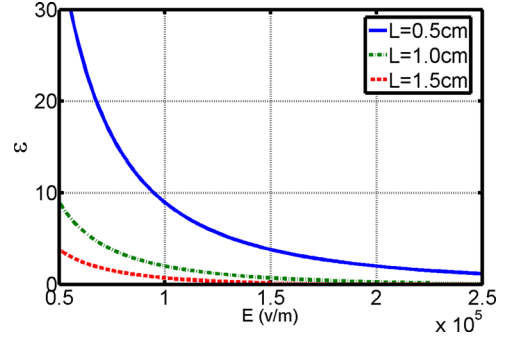


FIG. 3. The ratio ε of two eigenvectors in the nonmaximally entangled state could be easily modulated by the field E applied to region I. The blue solid line corresponds to the case where the length L of region I is 0.5 cm; while the green dashed-dotted line and the red dashed line correspond to $L = 1$ cm and $L = 1.5$ cm, respectively.

where we have $\varepsilon = \xi \Gamma_{101} / \Gamma_{110}$. Through the correlations between ξ and the applied field E , ε could be directly modulated by E . The values of ε are plotted as a function of E in Fig. 3 for different lengths of region I. From the figure, we find that ε decreases with increasing E . That effect is caused by the increasing of the EO coupling coefficient, which drives more light into the e -polarized state. Furthermore, the entanglement degree of the source is determined by the value of ε ; this relationship could be expressed by the concurrence¹⁹

$$C(\varphi) = \langle \varphi | \sigma_y \otimes \sigma_y | \varphi \rangle = \frac{2\varepsilon}{1 + \varepsilon^2}. \quad (6)$$

This means that we could conveniently control the entanglement degree of the source through modulation of E . That effect is illustrated in Fig. 4. For an arbitrary region length, the concurrence C of the entangled source could be changed between 0 and 1 by appropriate choice of E . Additionally, the fast response character of the EO process¹³ presents this kind of entangled state plenty of potential uses in practical applications.

In fact, our proposal for preparing the nonmaximally mode-entangled photon state is just a simple example of generating and manipulating of entangled states. The domain-engineered LN waveguide provides a very promising platform for this task through cascaded or coupled photon interaction processes.^{20,21} Based on SPDC, we could obtain initial entangled pairs, and the EO effect could be used to modulate certain photons in the pairs. In theory, we

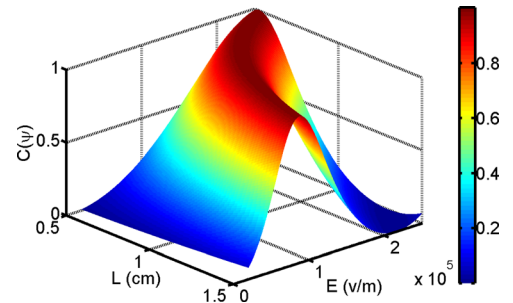


FIG. 4. The concurrence $C(\psi)$, which represents the entanglement degree of the source, can be conveniently modulated between 0 and 1 (the total range of C) by changing the field E applied to region I and the length L of region I.

could produce entangled states of any formation through this approach. Another possible example is the mixed state entanglement.²² We could realize it through introducing temporal decoherence²³ into nonmaximal entanglement with EO modulation. Besides the uniform domain periods we described above, the domain structure of LN could be elaborately prepared in more flexible patterns, for instance, quasi-periodic structures. These structures could provide more reciprocal vectors to compensate the multi-process phase mismatch with high efficiency.²⁴

In summary, we propose the generation of the nonmaximally mode-entangled photon state in an integrated circuit. The system is designed based on a domain-engineered LN waveguide. This scheme supplies the functions of integrated quantum systems and advances one step toward future practical large-scale quantum integrated circuits. Further, the entangled source could be modulated quickly and effectively through EO interaction, which makes it valuable for practical applications.

This work was sponsored by 973 programs (Nos. 2011CBA00205 and 2012CB921803), National Science Fund for Distinguished/Excellent Young Scholars (Nos. 61225026 and 61322503), and the Program for Changjiang Scholars and Innovative Research Team in University with Contract No. IRT13021.

¹P. G. Kwiat, K. Mattle, H. Weinfurter, A. Zeilinger, A. V. Sergienko, and Y. H. Shih, *Phys. Rev. Lett.* **75**, 4337 (1995).

²H. Takesue, K. Inoue, O. Tadanaga, Y. Nishida, and M. Adobe, *Opt. Lett.* **30**, 293 (2005).

³H. Y. Leng, X. Q. Yu, Y. X. Gong, P. Xu, Z. D. Xie, H. Jin, C. Zhang, and S. N. Zhu, *Nat. Commun.* **2**, 429 (2011).

⁴A. Politi, M. J. Cryan, J. G. Rarity, S. Yu, and J. L. O'Brien, *Science* **320**, 646 (2008).

⁵L. Sansoni, F. Sciarrino, G. Vallone, P. Mataloni, A. Crespi, R. Ramponi, and R. Osellame, *Phys. Rev. Lett.* **105**, 200503 (2010).

⁶B. J. Metcalf, N. T. Peter, J. B. Spring, D. Kundys, M. A. Broome, P. C. Humphreys, X. M. Jin, M. Barbieri, W. S. Kolthammer, J. C. Gates, B. J. Smith, N. K. Langford, P. G. R. Smith, and I. A. Walmsley, *Nat. Commun.* **4**, 1356 (2013).

⁷A. G. White, D. F. V. James, P. H. Eberhard, and P. G. Kwiat, *Phys. Rev. Lett.* **83**, 3103 (1999).

⁸M. Y. Ye, Y. S. Zhang, and G. C. Guo, *Phys. Rev. A* **69**, 022310 (2004).

⁹Z. Zhao, J. W. Pan, and M. S. Zhan, *Phys. Rev. A* **64**, 014301 (2001).

¹⁰J. Modlawska and A. Grudka, *Phys. Rev. Lett.* **100**, 110503 (2008).

¹¹A. Politi, J. C. F. Matthews, M. G. Thompson, and J. L. O'Brien, *IEEE J. Sel. Top. Quantum Electron.* **15**, 1673 (2009).

¹²Y. X. Gong, P. Xu, J. Shi, L. Chen, X. Q. Yu, P. Xue, and S. N. Zhu, *Opt. Lett.* **37**, 4374 (2012).

¹³Y. Q. Lu, Z. L. Wan, Q. Wang, Y. X. Xi, and N. B. Ming, *Appl. Phys. Lett.* **77**, 3719 (2000).

¹⁴A. Martin, O. Alibart, M. P. De Micheli, D. B. Ostrowsky, and S. Tanzilli, *New J. Phys.* **14**, 025002 (2012).

¹⁵M. F. Saleh, G. Di Giuseppe, B. E. A. Saleh, and M. C. Teich, *IEEE Photonics J.* **2**, 736 (2010).

¹⁶J. Lugani, S. Ghosh, and K. Thyagarajan, *Opt. Lett.* **37**, 3729 (2012).

¹⁷M. F. Saleh, B. E. A. Saleh, and M. C. Teich, *Phys. Rev. A* **79**, 053842 (2009).

¹⁸T. Suhara, *IEEE J. Quantum Electron.* **41**, 1203 (2005).

¹⁹Y. Ming, Z. J. Wu, A. H. Tan, X. K. Hu, F. Xu, and Y. Q. Lu, *AIP Adv.* **3**, 042122 (2013).

²⁰G. Assanto, G. I. Stegeman, M. Sheik-Bahae, and E. VanStryland, *IEEE J. Quantum Electron.* **31**, 673 (1995).

²¹G. Assanto, I. Torelli, and S. Trillo, *Opt. Lett.* **19**, 1720 (1994).

²²M. Barbieri, F. De Martini, G. Di Nepi, and P. Mataloni, *Phys. Rev. Lett.* **92**, 177901 (2004).

²³N. A. Peters, J. B. Altepeter, D. Branning, E. R. Jeffrey, T. C. Wei, and P. G. Kwiat, *Phys. Rev. Lett.* **92**, 133601 (2004).

²⁴S. N. Zhu, Y. Y. Zhu, and N. B. Ming, *Science* **278**, 843 (1997).